ChemPlusChem

Research Article
doi.org/10.1002/cplu.202200068

Chemistry Europe
European Chemical Societies Publishing

www.chempluschem.org

Structurally Constrained MUC1-Tn Mimetic Antigen as Template for Molecularly Imprinted Polymers (MIPs): A Promising Tool for Cancer Diagnostics

Pasquale Palladino[+], Francesco Papi[+], Maria Minunni, Cristina Nativi,* and Simona Scarano*[a]

Abnormal glycoconjugates have distinctly been recognized as potential biomarkers for cancer diagnosis. A great deal of attention has been focused on Tn antigen, an oversimplified mucin-1 *O*-glycan, over-expressed in different cancers. Herein, we investigate the possibility to replace the use of anti-Tn monoclonal antibodies with an innovative class of catecholamine-based Molecularly Imprinted Polymers (MIPs), emerging in recent years as promising tools for bioanalytical applications. MIPs are synthetic receptors characterized by high sensitivity and specificity towards the imprinted target. Here, original polynorepinephrine-based MIPs coupled to Surface Plasmon Resonance biosensing for Tn antigen recognition are reported. We have verified the imprinting and binding capacity of these MIPs towards very small antigenic entities, represented by the natural Tn antigen and the TnThr mimetic **1** (conjugated to BSA or linked to a MUC1 hexapeptide analogue), and compared the biosensor performances with an anti-Tn monoclonal antibody. The results clearly display the effectiveness of the pursued imprinting strategies.

Introduction

Tumor diseases are among the most common causes of death and the incidence rate is on the rise because in the next 10 years WHO foresees more than 20 million new cancer cases. With this perspective, it is worldwide accepted that early diagnosis is the key to get a more favorable cancer prognosis and to reduce its associated mortality.[1] As a matter of fact, cancers in adult patients generally take 20 to 30 years to develop late-stage disease, thus the opportunity to detect cancers before the onset of metastasis is realistic.[2] Ideally, cancer diagnostics should be non- or minimally invasive, thus new diagnostic tools to screen tumor biomarkers in urine, blood or serum became a matter of intense research.[3] At present, apart from very few exceptions,[2] established cancer biomarkers are not used for disease diagnostics because of high false negative and false positive results generally obtained.[4] Therefore, alternative cancer biomarkers detectable in body fluids (liquid biopsies) are extensively searched, including antibodies against aberrant glycans expressed on cancer cells.[5]

Carbohydrates are the most abundant biomolecules; connected by glycosidic linkages, they form glycoconjugates (i.e., glycoproteins, glycolipids, glycosphingolipids) which surround all cells. Abnormal glycoconjugates have distinctly been marked in many tumors (Tumor Associated Carbohydrate Antigens, TACAs) and recognized as potential biomarkers for cancer diagnosis.[6] Among TACAs, a great attention has been focused on Tn neoantigen. Tn is an over-simplified mucin-1 (MUC1) O-glycan formed by an aberrant truncated glycosylation. Mucins are highly O-glycosylated proteins largely expressed by healthy epithelial cells and deputed to lubricate tissues.[7] Structurally, Tn is an N-acetyl galactosamine linked through an α-O-glycosidic linkage to residues of serine or threonine (GalNAcα1-O-Ser/Thr, Figure 1), possible glycosylation sites of MUC1 20 amino acids tandem repeats (AHGVTSAPDTRPAPGSTAPP). Tn is over-expressed in different cancers (70–90% in lung, breast, stomach, and prostate) whereas little or no expressed on normal tissues.[8] Tn has been detected in early-tumor stages and its expression level is associated with tumor invasiveness and metastasis.[9,10] The result of aberrant glycosylation of MUC1 and consequent secretion of abnormal glyco-forms into the bloodstream, is the expression of anti-glycan antibodies. Although anti-Tn auto-antibodies can also be found in healthy subjects,[11] their statistical increase in tumor bearing hosts has recently been proposed as a tool for new early stage cancer diagnostics by indirect ELISA assays.[12,13] It is worthy of noting that the multivalent presentation of the Tn antigen has been proven an effective way to gain anti-Tn Abs recognition in Surface Plasmon Resonance (SPR) screenings.[14,15]

By a combined approach, multiple copies of the structurally rigid TnThr mimic **1** reported in Figure 1,[16,17] have been presented in a multivalent fashion by conjugation to the carrier protein CRM_{197} (Cross Reactive Material 197). The benefit of the multivalent approach was assessed by SPR technology, compar-

[a] *Dr. P. Palladino,[+] Dr. F. Papi,[+] Prof. M. Minunni, Prof. C. Nativi, Prof. S. Scarano*
Department of Chemistry, DICUS
University of Florence
via della Lastruccia 3–13, 50019 Sesto F.no (FI) (Italy)
E-mail: cristina.nativi@unifi.it
simona.scarano@unifi.it

[+] *These authors contributed equally to this work.*

Supporting information for this article is available on the WWW under https://doi.org/10.1002/cplu.202200068

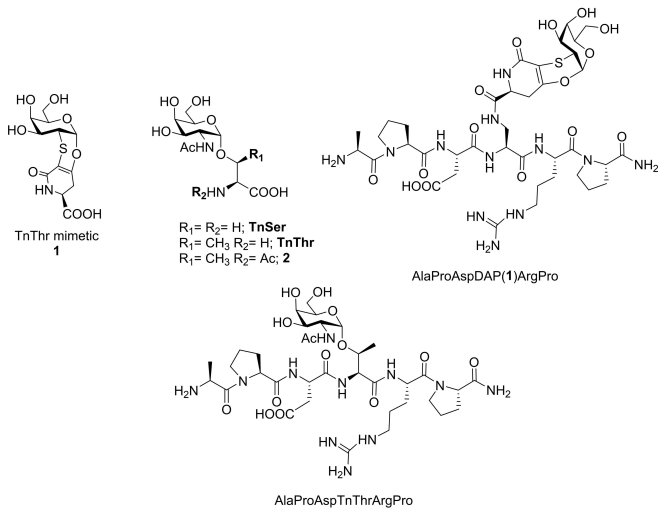

Figure 1. Structure of the Tn antigen linked through an α-O-glycosidic linkage to serine (TnSer) or threonine (TnThr), TnThr mimetic **1** (Tn_mime **1**), N-acetylated natural TnThr **2**, hexapeptides AlaProAspDAP(**1**)ArgPro (APD**1**RP) and AlaProAspThr(Tn)ArgPro (APDTTnRP). DAP = 2,3-diaminopropionic acid.

ing the natural and mimetic antigenic activity in terms of K_D.[18] Results displayed not only that the TnThr mimetic **1** retains an affinity constant comparable to the natural Tn ($K_D = 16.0$ mM and 12.5 mM, respectively) but also that its multivalent presentation on the CRM_{197} surface (four residues of mimetic **1** were displayed by CRM) yielded a $K_D = 11.5$ μM. This result attested the accessibility of the mimetic to a commercially available anti-Tn monoclonal antibody (Tn218 clone) and showed a 10^3-folds improvement.

In this work, we explored for the first time the possibility to replace the use of anti-Tn monoclonal antibodies (mAbs) with an innovative class of Molecularly Imprinted Polymers (MIPs), or 'plastic Abs', based on catecholamines (CAs) functional monomers, here norepinephrine (NE). Produced through several strategies, MIPs combine rapidity, simplicity, stability and cost effectiveness. In general, molecular imprinting is a process where the target molecule (i.e., the antigen) is used as a template, around which one or more functional monomers polymerize incorporating it in the polymeric network.[19] After the polymerization, the template is removed, leaving cavities that are complementary to the template, for shape, size and orientation. MIP is then able to selectively rebind the target molecule, generally thanks to the formation of non-covalent bonds. MIPs are characterized by high sensitivity and specificity toward the target, which allow the development of robust materials able to mimic natural recognition entities, including antibodies and receptors. Although molecular imprinting technology emerged more than two decades ago, its effective use in bioanalytical applications for antibody-free platforms encountered a series of failures. However, recently, a new class of endogenous functional monomers, belonging to the class of catecholamines (CAs), has been successfully tested to produce MIPs against a variety of targets, including proteins, and coupled to different bioanalytical platforms.[20–24] Thanks to its capacity to easily self-polymerize under mild alkaline conditions forming adherent films on virtually all the surfaces,[25] polydopamine (PDA) is undoubtedly the leading example within polycatecholamines (pCAs). Indeed, following pioneering investigations and applications,[26–28] it has generated an impressive amount of data ranging from material sciences, to bioanalytics and biosensing.[29–32] More recently, we unprecedentedly investigated NE, a natural neurotransmitter like DA and with the same polymerization capacity, as functional monomer for the imprinting of different biomarkers.[22–24] Notably, we observed that the binding performances and the related analytical parameters of imprinted polynorepinephrine (PNE) are even superior to those of PDA. Moreover, PNE may successfully reduce non-specific adsorption onto the MIP, thanks to its higher hydrophilicity with respect to PDA.[19,22–24] This kind of MIPs, likely the first MIPs to have a real prospect of success, shares with Abs an epitope-like recognition mechanism. This means that PDA- and PNE-based MIPs can be prepared by following a so-called 'epitope approach', that involves the imprinting of just a small portion of the target protein, mimicking the epitope/paratope natural scheme of Abs. In this scenario, here we report on the preparation of an innovative anti-TnThr mimetic PNE-based MIP coupled to SPR transduction. In this work we aim to verify the binding capacity of these MIPs vs. very small antigenic entities, which often show poor immunogenicity, here the native TnThr antigen (**2**, Figure 1) and the TnThr mimetic **1**, and compare the biosensor performances with a classical mAb available on the market. Moreover, the mimetic **1** was evaluated for its binding ability to the MIPs both when presented in a monovalent, or multivalent fashion by conjugation to BSA. As a monovalent antigen, we tested **1** linked to the hexapeptide AlaProAspDAP(**1**)ArgPro (APD**1**RP), an analogue of MUC1 tandem repeats (see above). MIPs were also imprinted with the N-acetylated natural TnThr **2**, and with the immunogenic MUC1 peptide domain linked to native Tn (AlaProAspThr(Tn)ArgPro, APDTTnRP), to evaluate the best combination in terms of binding affinity. In fact, although the binding concerns the glycan determinants (normally a monosaccharide or disaccharide moiety) it is possible that protein residues or lipid groups interact with Abs, interfering with the binding. This is particularly common with small or truncated *O*-glycans like the Tn antigen.

Results and Discussion

Synthesis of antigen mimetic 1 constructs. To evaluate the scaffold effect on TnThr mimetic **1** MIPs recognition, two constructs were synthesized. BSA was selected as a model of carrier protein substrate and lysines were decorated with 37 residues of **1** through a linker containing an activated carboxylic acid (Scheme 1). Tn_mime[37]BSA derivatization was confirmed by MALDI analysis (Figure S1).

To mimic natural MUC-1 tandem repeat sequence, the covalent coupling of acetylated TnThr mimetic **1** with hexapeptide AlaProAspDAPArgPro was run under solid-phased condensation standard conditions (PyBOP, DIPEA, DMF). After resin

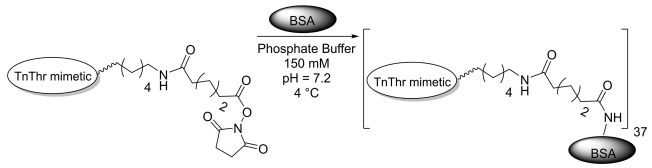

Scheme 1. Schematic representation of BSA glycosylation with TnThr mimetic **1** to give Tn_mime[37]BSA.

cleavage under acid conditions (TFA/TIS/H_2O) and deacetylation (NH_3 in MeOH), AlaProAspDAP(**1**)ArgPro (APD**1**RP, see Figure 1) was purified by C18 reversed-phase chromatography.

Evaluation of the affinity constant of Tn_mime[37]BSA by immuno-based SPR. As a reference, a classical immuno-based SPR biosensor was set up by immobilizing a commercially available mAb, namely Tn218, on CM5 chips, as previously reported.[18] The binding ability of Tn_mime[37]BSA was estimated by calibrating the antigen mimetic **1** presented in a multivalent fashion within the 21.3 × μM and 0.263 × μM concentration range. All experiments were run in triplicate and the results reported in Figure 2. It was not possible to reach the signal saturation because of large K_D values requiring higher experimental concentration range. However, this did not affect the accuracy of the extrapolated apparent $K_D = 11 \pm 5$ μM, which is in agreement with the reported affinity value ($K_D =$ 11.5 μM) of Tn218 for Tn mimetic **1** when conjugated to the carrier protein CRM_{197} (four residues of **1**, Tn_mime[4]CRM).[18]

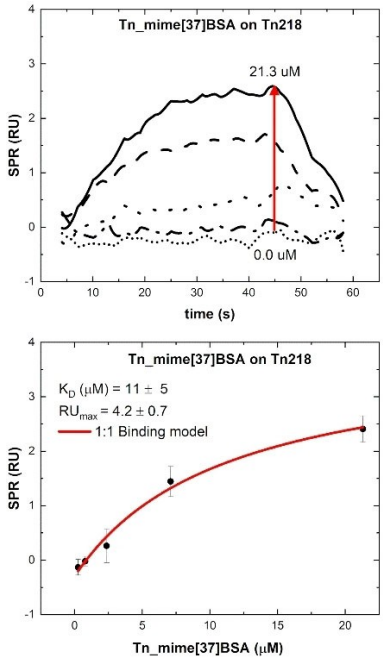

Figure 2. Upper panel: SPR analysis of Tn_mime[37]BSA affinity for Tn218 mAb immobilized on CM5 chip. Representative sensorgrams from binding experiments in triplicate for each concentration of a serial dilution (dilution factor 3) of Tn_mime[37]BSA from 0.263 × μM to 21.3 × μM. Lower panel: 1 : 1 binding curve for SPR signals (mean ± SD, n = 3) from all the associated sensorgrams.

PNE-based MIP for recognition of Tn antigen in Tn_mime[37]BSA. The natural TnThr antigen **2**, and the structurally related TnThr mimetic **1**, were used as imprinting templates to produce two different PNE-based MIPs on SPR gold chips (Figure 3). The binding ability of Tn_mime[37]BSA towards each MIP, working as an antibody mimetic, was estimated by SPR analysis on Tn_mime[37]BSA injection up to 8.0 μM. Considering the much larger SPR signals obtained for binding on MIPs, in these experiments we used a lower concentration range to save material. However, accurate results were obtained irrespective of such difference for analyte concentration. The results are reported in Figure 3, Table 1, and Figure S2 (see Supporting Information). Although it was not possible to reach a plateau for the SPR signal within the experimental concentration range, the extrapolated apparent K_D values indicate a close but larger affinity of TnThr mimetic **1** for MIP ($K_D = 4.3 \pm 1.4$ μM) with respect to natural TnThr **2** ($K_D = 11 \pm 2$ μM). Notably, both K_D values are comparable, or even lower, than the value found for the anti-Tn monoclonal antibody Tn218 (see above), showing the effectiveness of PNE-based molecular imprinting strategy in imprinting/recognizing monovalent, low molecular weight

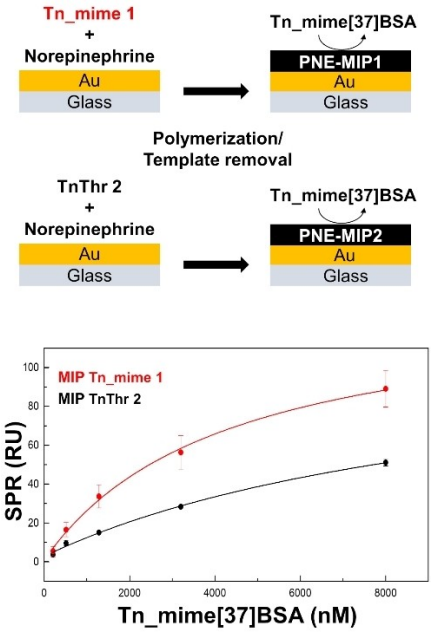

Figure 3. SPR analysis of Tn_mime[37]BSA affinity for PNE-MIP. Schematic representation of PNE imprinting and MIP formation for TnThr mimetic **1** and natural TnThr **2** (upper panel). SPR signals (mean ± SD, n = 3) and binding curves (1 : 1 fitting) for Tn_mime[37]BSA SPR from serial dilution (dilution factor 2.5) of Tn_mime[37]BSA from 0.205 × μM to 8.00 × μM onto PNE-MIP surfaces **1** and **2** (lower panel). SPR sensorgrams are reported in Figure S2 (see Supporting Information).

Table 1. Tn_mime[37]BSA affinity for TnThr-PNE-MIPs from SPR analysis and relative fitting parameters (mean ± SD, n = 3)

Analyte	MIP template	K_D [μM]	R_{MAX} [RU]
Tn_mime[37]BSA	mimetic **1**	4.3 ± 1.4	134 ± 15
Tn_mime[37]BSA	antigen **2**	11.0 ± 2.0	113 ± 13

glycans. This unprecedented evidence opens encouraging perspectives in this field.

PNE-based MIP for recognition of TnThr antigen in MUC1 tandem repeats. We further investigated the recognition capability of PNE-based MIP towards TnThr antigen when it is monovalently linked to the MUC1 hexapeptide domain APDTTnRP and its analogue APD**1**RP (see Figure 1). In contrast with data obtained for the antigen mimetic **1**, multivalently displayed by BSA, the two glycosyl hexapeptides did not show a relevant binding to MIPs imprinted nor with TnThr mimetic **1** or with natural TnThr **2** (see Figure 1). We speculate that such SPR results may depend on multivalency, fully solvent exposure, and on the larger mass of BSA (see Scheme 1) with respect to short peptides displaying a residue of native antigen or antigen mimetic, directly linked to the peptide backbone (see Figure 1). Accordingly, we decided to apply the PNE-MIP strategy to the entire glycosyl hexapeptides APD**1**RP and APDTTnRP instead of imprinting the simple monosaccharides (i.e., **1** and **2** respectively). This approach retraces the 'epitope imprinting' design for protein detection via MIPs recognition and it is here attempted for the first time by using a catecholamines-based MIP as an original *glycosylated-epitope imprinting* approach. Figure 4 shows the results of SPR analyses on PNE-modified gold chips. As reported in Figure 4A, both peptides at 4.00 μM gave good response signals on MIP obtained imprinting APD**1**RP. Interestingly, neither the natural nor the mimetic hexapeptides gave a relevant SPR signal increase when injected, under the same conditions, on the MIP obtained imprinting APDTTnRP (Figure S3, see Supporting Information). These different imprinting results may depend on better interactions during polymerization of catechol residues of norepinephrine with the rigid saccharide mimetic **1** of APD**1**RP with respect to the native Tn residue of APDTTnRP. Furthermore, SPR signals are very low (close to zero), and within the error, when the natural or the mimetic hexapeptide are injected on not-imprinted PNE (NIP) (Figure 4B), confirming the selectivity of the observed binding. Figure 4C shows the SPR curves fitting, and the correspondent fitting parameters are reported in Table 2. Here the affinity towards MIP surface, for both the hexapeptides tested, appears even stronger than the one observed between Tn_mime[37]BSA and Tn218 mAb or sugar-based MIP (see above), resulting in the submicromolar range. Taken together, these results from MIP and NIP suggest that the peptide APD**1**RP, displaying the constrained mimetic **1**, is able to generate a specific recognizing surface for Tn antigen as occurring in natural MUC1 tandem repeats.

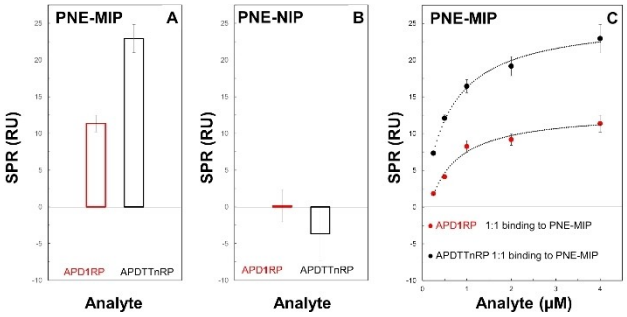

Figure 4. SPR analysis of MUC1 tandem repeats analogues affinity for PNE-MIP. (A) APD**1**RP (red) and APDTTnRP (black) hexapeptides injected at 4.0 μM on MIP obtained from APD**1**RP imprinting (mean ± SD, n = 3). (B) APD**1**RP (red) and APDTTnRP (black) hexapeptides injected at 4.00 μM on NIP (mean ± SD, n = 3). (C) SPR binding curves (1 : 1 fitting) for serial dilution (dilution factor 2) of APD**1**RP (red) and APDTTnRP (black) injected up to 4.00 μM onto the MIP surface obtained from APD**1**RP imprinting (mean ± SD, n = 3). SPR sensorgrams are reported in Figure S3 (see Supporting Information).

Table 2. MUC1 hexapeptides affinity for APD**1**RP-PNE-MIPs from SPR analysis and relative fitting parameters (mean ± SD, n = 3).

Analyte	MIP template	K_D [μM]	R_{MAX} [RU]
APD**1**RP	APD**1**RP	0.46 ± 0.19	17 ± 2
APDTTnRP	APD**1**RP	0.56 ± 0.19	26 ± 2

Recent studies indicated that GalNAcThr (TnThr) is rather rigid in solution and the sugar almost perpendicular to the peptide, while GalNAcSer (TnSer) is more flexible, and the GalNAc moiety parallel to the peptide.[36] Conformational studies in the solid state showed that the substitution of Thr by Ser within the recognition epitope of the MUC1 glycopeptide [APDT/S(α-O-GalNAc)RP] resulted in the reduction of the binding affinity vs. the golden standard anti-MUC1 antibody, SM3.[35] Some years ago, we synthesized a conformationally locked mimetic of TnThr antigen, namely **1**, with increased stability to glycosidases.[16,17] The TnThr mimetic **1** (see Figure 1) was suitably functionalized to be multivalently conjugated to macromolecular constructs, thus increasing the availability for biological counterparts. In particular, we decorated the adjuvant CRM_{197} with multiple residues of mimetic **1**, proving the ability of the glycoprotein so obtained to bind to anti-Tn antibody Tn218 and elicit in vivo a protective immune response.[18] The soundness of **1** to mimic the TnThr determinant, prompted us to synthesize **1**-imprinted polymers. To the best of our knowledge, there are very few examples of glycans and glycoconjugates used as templates for catecholamine-based molecular imprinting in the literature, and only referred to the use of PDA.[37–39] Such paucity of experimental studies, despite the large literature on polydopamine, somehow suggested to test the more hydrophilic polynorepinephrine for sugar imprinting.[22–24] Accordingly, our preliminary studies employed mimetic and natural Tn antigens (**1** and **2** respectively, see Figure 1) as templates for MIPs, and Tn_mime[37]BSA as a model of multivalent glycoprotein. The latter is useful for SPR signal detection working as mass enhancer and offering larger affinity, due to multivalency, with respect to monovalent Tn antigen.

Conclusion

The results here reported showed the effectiveness of PNE-based molecular imprinting strategy also for glycans recognition, indicating an affinity of Tn_mime[37]BSA for PNE-MIPs in the micromolar range (Figure 3, Table 1), which is comparable, or even lower, than the affinity for the anti-Tn mAb, Tn218 (Figure 2). Moreover, focusing on the native MUC1 epitope peptide APDTRP, and on the threonine-glycosylated derivative, which are masked in healthy cells but became accessible in cancer cells and exposed to immune system,[36] we used the glycopeptides APDTTnRP (as control) and APD**1**RP (native Tn is replaced with Tn mime, **1** see Figure 1) as template to prepare PNE-MIPs and bind the Tn antigen in MUC1 tandem repeats. Both the peptides gave good SPR signals only on the PNE-MIP imprinted with the APD**1**RP epitope (Figure 4, Table 2). More importantly, it has been shown that the affinity towards this MIP surface for both the peptides is in the submicromolar range, i.e., stronger than the interaction recorded between Tn_mime[37]BSA and the antibody imprinted (see Figure 3). These results suggest that the rationally designed peptide APD**1**RP for epitope imprinting with PNE enabled to generate a specific recognizing surface for naturally occurring MUC1 antigen, potentially offering a new tool for cancer diagnostics. The peculiar effectiveness of the Tn antigen mimetic **1** for PNE-based imprinting, as monovalent construct (see Figure 3) or linked to MUC1 hexapeptide (APD**1**RP) appears related to its locked structure that may allow better interactions between the rigid saccharide mimetic with catechol moiety of norepinephrine during polymerization, with respect to the flexible natural residue. This intriguing aspect requires further investigation and is the object of ongoing research. In conclusion, the paucity of effective cancer biomarkers safely used as diagnostics and the vast majority of detected neoantigens which are patient-specific, or "private", highlight the need of personalized diagnostic strategies and make the PNE-based MIPs deserving of attention as potential tailored-made diagnostic tools.

Experimental Section

BSA glycosylation with mimetic 1. A 0.8 mM solution of BSA in NaPi, buffer (150 mM, pH 7.2 buffer) was treated with 50 equiv. of activated TnThr mimetic **1**.[18] The reaction mixture was incubated at 4 °C for 24 h under shaking (Scheme 1). The success of the reaction was proved by an SDS-PAGE. The conjugate was then purified from unreacted sugar by multistep washings with water using a 10 kDa MWCO membrane centrifugal device (Millipore). About 37 synthetic glycans were grafted to BSA (Tn_mime[37]BSA) as estimated by TNBS assay and confirmed by MALDI UltraFlex III analysis (see Supporting Information, Figure S1, Table S1).

Glycosylation of hexapeptide AlaProAspDAPArgPro with mimetic 1. Glycopeptide APD**1**RP was synthesized by coupling of mimetic **1** to the hexapeptide AlaProAspDAPArgPro protected and linked to the resin, with PyBOP and DIPEA in DMF (Scheme 2). After 2 h, the resin was washed with DMF and the acetylated glycopeptide was detached and deprotected by acidolysis reaction (TFA/TIS/H_2O 95:2.5:2.5) followed by treatment with NH_3 in MeOH 1 M. Glycopeptide APD**1**RP was purified by C18 reversed-phase chromatography (H_2O/CH_3CN 80:20) and characterized by NMR and HRMS.[18] ESI-HRMS m/z (%): calculated, $[M+H]^+ = 955{,}3938$; found, 955.39298 (100) $[M+H]^+$.

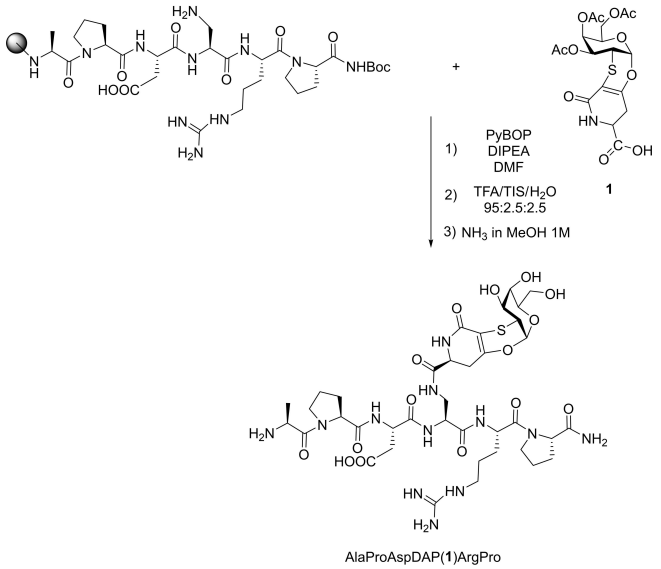

Scheme 2. Glycosylation of hexapeptide AlaProAspDAPArgPro with Tn mime **1** to give APD**1**RP.

Immobilization of Tn218 mAb on chips. Anti-Tn antibody (Tn218 mAb) was immobilized onto flow cell 2 of a carboxymethyl dextran matrix (CM5, Cytiva) following the amino coupling reaction protocol. Briefly, after an activation step with 50 mmol L^{-1} NHS and 200 mmol L^{-1} EDAC (contact time: 420 s, flow rate: 10 μL min^{-1}) for both flow cell 1 (reference channel) and flow cell 2 (working channel), the dextran matrix of flow cell 2 only was modified with Tn218 mAb (contact time: 420 s, 10 μg mL^{-1} in 10 mmol L^{-1} acetate buffer, pH 4.0 selected by a 'pH scouting' (Biacore X100 Handbook BR-1008-10 Edition AC.), followed by the deactivation of the surface for both channels with ethanolamine (contact time: 420 s, 10 μg mL^{-1}) (see Supporting Information, Figure S2).

PNE-based MIPs preparation. Anti-Tn MIPs were prepared via 'drop casting', i.e., by dropping directly on bare gold sensor chips (Cytiva) a solution containing the functional monomer (NE) and the selected template at 1 mM. After 5 h at 25 °C the polymerization is stopped, the template is removed by using acetic acid (5% v/v), and the sensor chip washed. A more detailed description of the imprinting method for a different template is reported in Torrini et al., 2021.[24] The binding features of the MIPs were evaluated by using the SPR platform, testing different concentrations of the analytes on the PNE MIP and measuring the relative affinities.

Acknowledgements

We thank Fondazione CR Firenze, project #24259-2018 for financial support. The authors are grateful to MIUR-Italy (Progetto Dipartimenti d'Eccellenza 2018–2022 allocated to Dipartimento di Chimica). Open Access Funding provided by Universita degli Studi di Firenze within the CRUI-CARE Agreement.

Conflict of Interest

The authors declare no conflict of interest.

Data Availability Statement

The data that support the findings of this study are available from the corresponding author upon reasonable request.

Keywords: biomarker · molecularly imprinted polymers · polynorepinephrine · surface plasmon resonance · TACA · Tn antigen mimetic

[1] F. Bray, J. Ferlay, I. Soerjomataram, R. L. Siegel, L. A. Torre, A. Jemal, *CA-Cancer J. Clin.* **2018**, *68*, 394–424.
[2] J. D. Cohen, L. Li, Y. Wang, C. Thoburn, B. Afsari, L. Danilova, C. Douville, A. A. Javed, F. Wong, A. Mattox, R. H. Hruban, C. L. Wolfgang, M. G. Goggins, M. Dal Molin, T.-L. Wang, R. Roden, A. P. Klein, J. Ptak, L. Dobbyn, J. Schaefer, N. Silliman, M. Popoli, J. T. Vogelstein, J. D. Browne, R. E. Schoen, R. E. Brand, J. Tie, P. Gibbs, H.-L. Wong, A. S. Mansfield, J. Jen, S. M. Hanash, M. Falconi, P. J. Allen, S. Zhou, C. Bettegowda, L. A. Diaz, C. Tomasetti, K. W. Kinzler, B. Vogelstein, A. M. Lennon, N. Papadopoulos, *Science* **2018**, *359*, 926–930.
[3] A. Blsakova, F. Kveton, P. Kasak, J. Tkac, *Expert Rev. Mol. Diagn.* **2019**, *19*, 1057–1068.
[4] J. Tkac, T. Bertok, M. Hires, E. Jane, L. Lorencova, P. Kasak, *Expert Rev. Proteomics* **2019**, *16*, 65–76.
[5] T. Pochechueva, S. Alam, A. Schötzau, A. Chinarev, N. V. Bovin, N. F. Hacker, F. Jacob, V. Heinzelmann-Schwarz, *J. Ovarian Res.* **2017**, *10*, 8.
[6] F. Hossain, P. R. Andreana, *Pharmaceuticals* **2019**, *12*, 84.
[7] F.-G. Hanisch, S. Muller, *Glycobiology* **2000**, *10*, 439–449.
[8] A. Tsuchiya, M. Kanno, T. Kawaguchi, Y. Endo, G.-J. Zhang, T. Ohtake, I. Kimijima, *Breast Cancer* **1999**, *6*, 175–180.
[9] M.-M. Wei, Y.-S. Wang, X.-S. Ye, *Med. Res. Rev.* **2018**, *38*, 1003–1026.
[10] C. Nativi, O. Renaudet, *ACS Med. Chem. Lett.* **2014**, *5*, 1176–1178.
[11] G. F. Springer, *J. Mol. Med.* **1997**, *75*, 594–602.
[12] V. J. Somovilla, I. A. Bermejo, I. S. Albuquerque, N. Martínez-Sáez, J. Castro-López, F. García-Martín, I. Compañón, H. Hinou, S. I. Nishimura, J. Jiménez-Barbero, J. L. Asensio, A. Avenoza, J. H. Busto, R. Hurtado-Guerrero, J. M. Peregrina, G. J. L. Bernardes, F. Corzana, *J. Am. Chem. Soc.* **2017**, *139*, 18255–18261.
[13] P. A. Guillen-Poza, E. M. Sánchez-Fernández, G. Artigas, J. M. García Fernández, H. Hinou, C. Ortiz Mellet, S.-I. Nishimura, F. Garcia-Martin, *J. Med. Chem.* **2020**, *63*, 8524–8533.
[14] C. Pifferi, A. Ruiz-de-Angulo, D. Goyard, C. Tiertant, N. Sacristán, D. Barriales, N. Berthet, J. Anguita, O. Renaudet, A. Fernández-Tejada, *Chem. Sci.* **2020**, *11*, 4488–4498.
[15] I. Compañón, A. Guerreiro, V. Mangini, J. Castro-López, M. Escudero-Casao, A. Avenoza, J. H. Busto, S. Castillón, J. Jiménez-Barbero, J. L. Asensio, G. Jiménez-Osés, O. Boutureira, J. M. Peregrina, R. Hurtado-Guerrero, R. Fiammengo, G. J. L. Bernardes, F. Corzana, *J. Am. Chem. Soc.* **2019**, *141*, 4063–4072.
[16] A. Ardá, R. Bosco, J. Sastre, F. J. Cañada, S. André, H.-J. Gabius, B. Richichi, J. Jiménez-Barbero, C. Nativi, *Eur. J. Org. Chem.* **2015**, *2015*, 6823–6831.
[17] B. Richichi, B. Thomas, M. Fiore, R. Bosco, H. Qureshi, C. Nativi, O. Renaudet, L. BenMohamed, *Angew. Chem. Int. Ed.* **2014**, *53*, 11917–11920; *Angew. Chem.* **2014**, *126*, 12111–12114.
[18] A. Amedei, F. Asadzadeh, F. Papi, M. G. Vannucchi, V. Ferrucci, I. A. Bermejo, M. Fragai, C. V. De Almeida, L. Cerofolini, S. Giuntini, M. Bombaci, E. Pesce, E. Niccolai, F. Natali, E. Guarini, F. Gabel, C. Traini, S. Catarinicchia, F. Ricci, L. Orzalesi, F. Berti, F. Corzana, M. Zollo, R. Grifantini, C. Nativi, *iScience* **2020**, *23*, 101250.
[19] L. Uzun, A. P. F. Turner, *Biosens. Bioelectron.* **2016**, *76*, 131–144.
[20] P. Palladino, M. Minunni, S. Scarano, *Biosens. Bioelectron.* **2018**, *106*, 93–98.
[21] P. Palladino, F. Bettazzi, S. Scarano, *Anal. Bioanal. Chem.* **2019**, *411*, 4327–4338.
[22] V. Baldoneschi, P. Palladino, M. Banchini, M. Minunni, S. Scarano, *Biosens. Bioelectron.* **2020**, *157*, 112161.
[23] V. Baldoneschi, P. Palladino, S. Scarano, M. Minunni, *Anal. Bioanal. Chem.* **2020**, *412*, 5945–5954.
[24] F. Torrini, P. Palladino, V. Baldoneschi, S. Scarano, M. Minunni, *Anal. Chim. Acta* **2021**, *1161*, 338481.
[25] F. Battaglia, V. Baldoneschi, V. Meucci, L. Intorre, M. Minunni, S. Scarano, *Talanta* **2021**, *230*, 122347.
[26] H. Lee, S. M. Dellatore, W. M. Miller, P. B. Messersmith, *Science* **2007**, *318*, 426–430.
[27] Y. Li, M. Liu, C. Xiang, Q. Xie, S. Yao, *Thin Solid Films* **2006**, *497*, 270–278.
[28] K. Liu, W.-Z. Wei, J.-X. Zeng, X.-Y. Liu, Y.-P. Gao, *Anal. Bioanal. Chem.* **2006**, *385*, 724–729.
[29] Y. Fu, L. Yang, J. Zhang, J. Hu, G. Duan, X. Liu, Y. Li, Z. Gu, *Mater. Horiz.* **2021**, DOI 10.1039/d0mh01985b.
[30] Z. Jin, L. Yang, S. Shi, T. Wang, G. Duan, X. Liu, Y. Li, *Adv. Funct. Mater.* **2021**, *31*, 2103391.
[31] Y. Tang, Y. Tan, K. Lin, M. Zhu, *Front. Chem.* **2021**, *9*, DOI 10.3389/fchem.2021.727123.
[32] P. Yang, F. Zhu, Z. Zhang, Y. Cheng, Z. Wang, Y. Li, *Chem. Soc. Rev.* **2021**, *50*, 8319–8343.
[33] D. M. Beckwith, M. Cudic, *Semin. Immunol.* **2020**, *47*, 101389.
[34] M. R. Pratt, C. R. Bertozzi, *Chem. Soc. Rev.* **2005**, *34*, 58.
[35] Y. Tachibana, G. L. Fletcher, N. Fujitani, S. Tsuda, K. Monde, S.-I. Nishimura, *Angew. Chem. Int. Ed.* **2004**, *43*, 856–862; *Angew. Chem.* **2004**, *116*, 874–880.
[36] N. Martínez-Sáez, J. Castro-López, J. Valero-González, D. Madariaga, I. Compañón, V. J. Somovilla, M. Salvadó, J. L. Asensio, J. Jiménez-Barbero, A. Avenoza, J. H. Busto, G. J. L. Bernardes, J. M. Peregrina, R. Hurtado-Guerrero, F. Corzana, *Angew. Chem. Int. Ed.* **2015**, *54*, 9830–9834; *Angew. Chem.* **2015**, *127*, 9968–9972.
[37] C.-H. Lu, Y. Zhang, S.-F. Tang, Z.-B. Fang, H.-H. Yang, X. Chen, G.-N. Chen, *Biosens. Bioelectron.* **2012**, *31*, 439–444.
[38] X. Qu, F. Wang, Y. Sun, Y. Tian, R. Chen, X. Ma, C. Liu, *RSC Adv.* **2016**, *6*, 86455–86463.
[39] T. Pan, Y. Lin, Q. Wu, K. Huang, J. He, *J. Sep. Sci.* **2021**, *44*, 2465–2473.

Manuscript received: February 25, 2022
Revised manuscript received: April 18, 2022
Accepted manuscript online: April 19, 2022

RESEARCH ARTICLE

A structurally constrained α-Tn antigen mimetic **1**, as monomer or linked to a MUC1 hexapeptide, has been selected as template to imprint polynorepinephrine (PNE). The imprinting and binding capacity of the PNE-MIPs so obtained have been screened towards very small antigenic entities, like the natural Tn antigen and the TnThr mimetic **1**, or towards **1** MUC1 hexapeptide analogues.

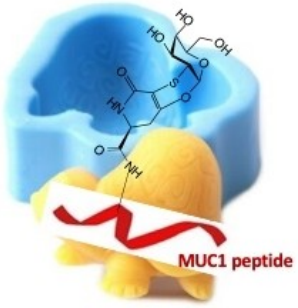

Dr. P. Palladino, Dr. F. Papi, Prof. M. Minunni, Prof. C. Nativi, Prof. S. Scarano**

1 – 7

Structurally Constrained MUC1-Tn Mimetic Antigen as Template for Molecularly Imprinted Polymers (MIPs): A Promising Tool for Cancer Diagnostics